Universality of electron accumulation at wurtzite *c*- and *a*-plane and zinc-blende InN surfaces

P. D. C. King, T. D. Veal, and C. F. McConville[a)]
Department of Physics, University of Warwick, Coventry, West Midlands CV4 7AL, United Kingdom

F. Fuchs, J. Furthmüller, and F. Bechstedt
Institut für Festkörpertheorie und -optik, Friedrich-Schiller-Universität, Max-Wien-Platz 1, D-07743 Jena, Germany

P. Schley and R. Goldhahn
Institut für Physik, TU Ilmenau, PF 100565, 98684 Ilmenau, Germany

J. Schörmann, D. J. As, and K. Lischka
Department Physik, Universität Paderborn, Warburger Strasse 100, 33098 Paderborn, Germany

D. Muto, H. Naoi,[b)] and Y. Nanishi
Department of Photonics, Ritsumeikan University, 1-1-1 Noji-Higashi, Kusatsu, Shiga 525-8577, Japan

Hai Lu[c)] and W. J. Schaff
Department of Electrical and Computer Engineering, Cornell University, Ithaca, New York 14853

(Received 2 July 2007; accepted 2 August 2007; published online 27 August 2007)

Electron accumulation is found to occur at the surface of wurtzite $(11\bar{2}0)$, (0001), and $(000\bar{1})$ and zinc-blende (001) InN using x-ray photoemission spectroscopy. The accumulation is shown to be a universal feature of InN surfaces. This is due to the low Γ-point conduction band minimum lying significantly below the charge neutrality level. © *2007 American Institute of Physics*.
[DOI: 10.1063/1.2775807]

InN is considered unusual among III-V semiconductors in that it exhibits electron accumulation at its surface,[1–3] the only other reported occurrence of this phenomena in III-V materials occurring in InAs.[4,5] The accumulation has been observed to be much more extreme in InN than InAs, explained in terms of the Γ-point conduction band minimum (CBM) in InN lying well below the charge neutrality level (CNL), or branch point energy.[6] Experimental studies to date have focused on wurtzite *c*-plane surfaces,[1–3,7] although previous first-principles calculations have predicted electron accumulation at nonpolar surfaces.[8] Here, we consider wurtzite *a*- and *c*-plane and zinc-blende (001) surfaces and demonstrate the universal nature of the electron accumulation. This is discussed in terms of the bulk band structure and CBM position relative to the CNL.

All samples were grown by plasma-assisted molecular beam epitaxy. The *c*-plane wurtzite samples were grown on *c*-plane sapphire substrates, with the In- and N-polarity [(0001) and $(000\bar{1})$, respectively] samples incorporating a GaN/AlN and low-temperature InN buffer layer, respectively. The *a*-plane $(11\bar{2}0)$ sample was grown on an *r*-plane $(1\bar{1}02)$ sapphire substrate incorporating a GaN/AlN buffer layer. The (001) zinc-blende sample was grown on an (001) 3*C*-SiC substrate incorporating a zinc-blende GaN buffer layer, resulting in an estimated 95% zinc-blende phase InN.[9] Details of the various growth methods are reported elsewhere. [9–12]

The x-ray photoemission spectroscopy (XPS) measurements were performed at room temperature using a Scienta ESCA300 spectrometer at the National Centre for Electron Spectroscopy and Surface Analysis, Daresbury Laboratory, UK. Details of the spectrometer are reported elsewhere.[13] The energy scale is given with respect to the Fermi level, calibrated using the Fermi edge of an ion-bombarded silver reference sample. The position of the valence band maximum (VBM) at the surface is often calculated by extrapolating a linear fit to the leading edge of the valence band photoemission.[14] However, in the presence of significant downward band bending, this technique is known to underestimate the true VBM to surface Fermi level separation;[13] it is therefore determined here as the shift in energy required to align the valence band photoemission spectra with quasiparticle-corrected density functional theory (QPC-DFT) calculations (using the HSE03 hybrid exchange-correlation potential) of the valence band density of states (VB-DOS) which, by convention, have the VBM at 0 eV. Details of the calculations are reported elsewhere.[15] For comparison with the experimental results, the QPC-DFT is broadened by a 0.2 eV full width at half maximum (FWHM) Lorentzian and a 0.45 eV FWHM Gaussian to account for lifetime and instrumental broadening, respectively.

Sample preparation in the XPS chamber was achieved by atomic hydrogen cleaning (AHC), which has been shown to effectively clean surfaces of InN (Ref. 16) without causing electronic damage. The AHC consisted of annealing the samples at ~200 °C under exposure to a 10–20 kL dose of molecular hydrogen passed through a thermal gas cracker with a cracking efficiency of approximately 50%, followed by a 1–2 h annealing at ~275 °C. Scanning electron microscopy was used to ensure that the AHC had not resulted in In-droplet formation at the surface.

[a)]Electronic mail: c.f.mcconville@warwick.ac.uk
[b)]Present address: Wakayama National College of Technology, 77 Nojima, Nada-Cho, Gobo, Wakayama 644-0023, Japan.
[c)]Present address: Department of Physics, Nanjing University, Nanjing, 210093, China

 © 2007 American Institute of Physics
Downloaded 27 Jan 2009 to 130.236.174.69. Redistribution subject to AIP license or copyright; see http://apl.aip.org/apl/copyright.jsp

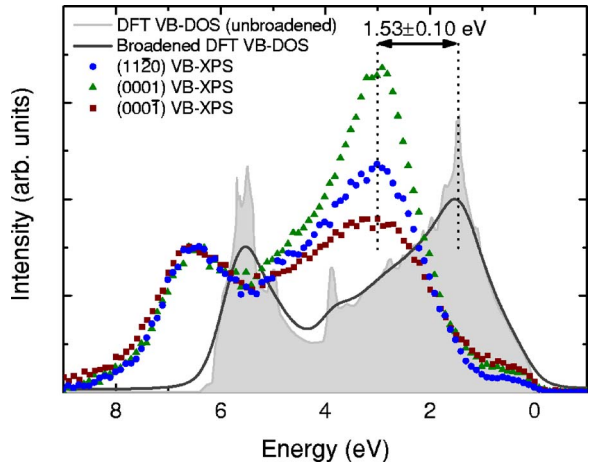

FIG. 1. (Color online) Valence band photoemission spectra for (11$\bar{2}$0), (0001), and (000$\bar{1}$) InN surfaces, relative to the Fermi level. QPC-DFT VB-DOS is shown without (shaded) and with lifetime and instrumental broadening. The indicated shift in peak position gives the VBM to surface Fermi level separation.

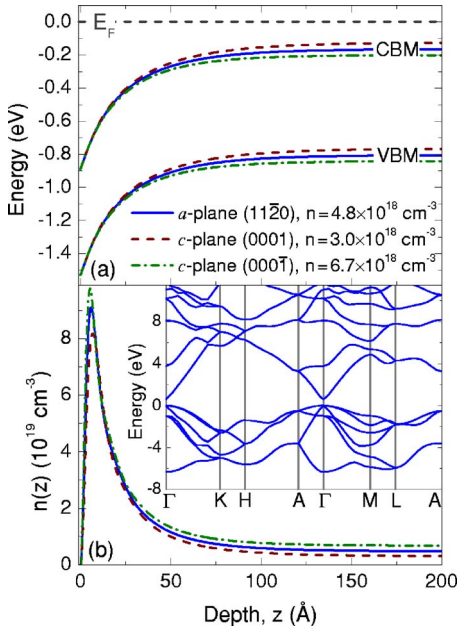

FIG. 2. (Color online) Band bending relative to the Fermi level (a) and resulting carrier concentration variation (b) in the accumulation layer at wurtzite InN surfaces. QPC-DFT bulk band structure calculations are shown inset.

The valence band photoemission spectra for the wurtzite samples are shown, with QPC-DFT VB-DOS calculations, in Fig. 1. All the photoemission spectra are coincident in energy, indicating the same VBM to surface Fermi level separation. This is determined, from the shift in peak position compared to the QPC-DFT calculations, to be 1.53±0.10 eV for all three samples. The differences in intensity of the ~3 eV peak between the samples have been shown to be a signature of the film polarity and the resulting contribution to the surface DOS.[7]

The position of the surface Fermi level, well above the CBM, indicates a downward band bending relative to the Fermi level at the surface, leading to electron accumulation for all wurtzite samples measured. To investigate this further, the band bending profile and corresponding electron accumulation in the surface space-charge region was determined by solving Poisson's equation numerically within the modified Thomas-Fermi approximation (MTFA) following the method described by Veal *et al.*[17] The MTFA correction has been shown[18] to yield profiles that are in good agreement with those obtained from full self-consistent Poisson-Schrödinger calculations. The resulting profiles are shown in Fig. 2, and the relevant parameters listed in Table I.

Despite differences in bulk Fermi level positions, the pinning of the surface Fermi level at the same energy for *a*-plane and both polarities of *c*-plane InN means that the band bending close to the surface is very similar [Fig. 2(a)], resulting in similar near-surface charge profiles [Fig. 2(b)]. Indeed, the calculated surface state density is the same for all samples (Table I) indicating the universality of the electron accumulation at wurtzite InN surfaces.

This universality can be understood by considering the bulk band structure of InN, shown inset in Fig. 2. The Γ-point CBM is located very low in energy compared to the average conduction band edge across the Brillouin zone (BZ). This means that the CNL, which occurs at approximately the average midgap energy over the entire BZ,[20] lies well above the Γ-point CBM. The CNL determines the energy at which surface states change their character from predominantly donor-like (below) to acceptor-like (above). Its location high above the CBM in InN results in unoccupied and hence positively charged donor surface states, which have donated their electrons into the conduction band, leading to a large accumulation of electrons near the surface and a downward band bending to maintain charge neutrality. While the exact microscopic nature of these surface states may vary between different surfaces, the bulk band structure dictates that electron accumulation will be present at all surfaces provided the bulk Fermi level lies below the CNL, explaining the universal nature of the electron accumulation observed here.

The valence band photoemission is shown for zinc-blende (001) InN in Fig. 3(a). The DOS is somewhat different for zinc-blende to wurtzite polymorphs, and the detailed agreement of the XPS with the QPC electronic structure calculations will be discussed elsewhere,[21] although good agreement is seen when incorporating a VBM to surface Fermi level shift of 1.38±0.10 eV.

Poisson-MTFA calculations for (001) InN, using a room temperature band gap of 0.56 eV (Ref. 9) and a band-edge electron effective mass of $0.039m_0$ [based on the empirical relation $m^* \approx 0.07E_g$ (Ref. 22)], are shown in Fig. 3. Due to growth on a conducting substrate, single field Hall effect measurements did not yield an accurate carrier concentration for the InN layer. The bulk Fermi level was therefore esti-

TABLE I. Bulk carrier density n, determined from single field Hall effect measurements, and corresponding bulk Fermi level above the CBM, E_{F_b}, calculated using Fermi-Dirac carrier statistics, and the α-approximation (Ref. 19) to account for conduction band nonparabolicity. The band bending V_{bb} is calculated from the relative surface and bulk Fermi level positions. Poisson-MTFA calculations give the surface state density N_{ss}.

Orientation	n (cm^{-3})	E_{F_b} (eV)	V_{bb} (eV)	N_{ss} (cm^{-2})
(11$\bar{2}$0)	4.8×10^{18}	0.164	−0.725	1.66×10^{13}
(0001)	3.0×10^{18}	0.124	−0.765	1.64×10^{13}
(000$\bar{1}$)	6.7×10^{18}	0.200	−0.689	1.65×10^{13}

Downloaded 27 Jan 2009 to 130.236.174.69. Redistribution subject to AIP license or copyright; see http://apl.aip.org/apl/copyright.jsp

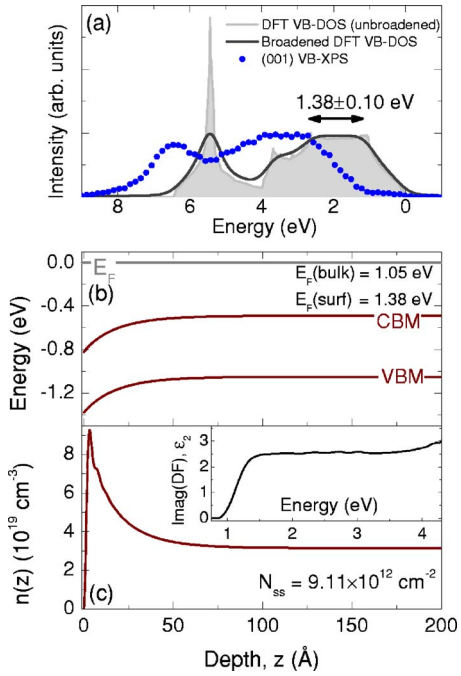

FIG. 3. (Color online) (a) Valence band photoemission spectra for (001) InN and zinc-blende QPC-DFT VB-DOS shown without (shaded) and with lifetime and instrumental broadening. Poisson-MTFA calculations yield band bending (b) and carrier concentration (c) profiles. The bulk Fermi level was determined from the imaginary part of the dielectric function, determined by spectroscopic ellipsometry (shown inset).

mated from the imaginary part of the dielectric function (determined by spectroscopic ellipsometry[9]), shown in the inset of Fig. 3, to be 1.05 eV above the VBM, corresponding to a bulk electron concentration (from carrier statistics) of 3.2×10^{19} cm^{-3}.

Despite the higher bulk carrier density than in the wurtzite samples, a distinct electron accumulation is still observed, although the Fermi level appears to pin slightly lower above the VBM and the surface state density from Poisson-MTFA calculations ($N_{ss}=9.11\times10^{12}$ cm^{-2}) is somewhat lower for the zinc-blende than the wurtzite cases. Although it has not been determined for InN, the valence band offset (VBO) between wurtzite and zinc-blende GaN is less than 100 meV,[23,24] and would be expected to decrease with increasing ionicity of the semiconductor.[25] Thus, the VBO between wurtzite and zinc-blende InN is expected to be small, and consequently the band edges in zinc-blende InN will still occur significantly below the CNL. Thus, while the detailed surface state distribution may be different to the previous cases, leading to the slight differences in observed surface Fermi level pinning position, the bulk band structure still dictates that electron accumulation will occur at the surface for this polymorph, as observed here.

In conclusion, we have shown that electron accumulation occurs universally at InN surfaces, due to the low Γ-point conduction band minimum lying significantly below the charge neutrality level. The surface Fermi level pinning was shown to be the same for *a*-plane and for both polarities of *c*-plane wurtzite InN, although the pinning was slightly lower for zinc-blende (001) InN.

The authors are grateful to D. Law and G. Beamson of NCESS for their assistance with XPS measurements and H. Nagasawa and M. Abe from SiC Development Center, HOYA Corporation, Japan for supplying the 3*C*-SiC substrates. The authors acknowledge the Engineering and Physical Sciences Research Council, UK, for support under Grant Nos. EP/C535553/1 and GR/S14252/01 and the Deutsche Forschungsgemeinschaft for support under Project No. Be1346/18-2.

[1] H. Lu, W. J. Schaff, L. F. Eastman, and C. E. Stutz, Appl. Phys. Lett. **82**, 1736 (2003).
[2] I. Mahboob, T. D. Veal, C. F. McConville, H. Lu, and W. J. Schaff, Phys. Rev. Lett. **92**, 036804 (2004).
[3] L. Colakerol, T. D. Veal, H.-K. Jeong, L. Plucinski, A. DeMasi, T. Learmonth, P.-A. Glans, S. Wang, Y. Zhang, L. F. J. Piper, P. H. Jefferson, A. Fedorov, T.-C. Chen, T. D. Moustakas, C. F. McConville, and K. E. Smith, Phys. Rev. Lett. **97**, 237601 (2006).
[4] D. C. Tsui, Phys. Rev. Lett. **24**, 303 (1970).
[5] M. Noguchi, K. Hirakawa, and T. Ikoma, Phys. Rev. Lett. **66**, 2243 (1991).
[6] I. Mahboob, T. D. Veal, L. F. J. Piper, C. F. McConville, H. Lu, W. J. Schaff, J. Furthmüller, and F. Bechstedt, Phys. Rev. B **69**, 201307(R) (2004).
[7] T. D. Veal, P. D. C. King, P. H. Jefferson, L. F. J. Piper, C. F. McConville, H. Lu, W. J. Schaff, P. A. Anderson, S. M. Durbin, D. Muto, H. Naoi, and Y. Nanishi, Phys. Rev. B **76**, 075313 (2007).
[8] C. G. Van de Walle and D. Segev, J. Appl. Phys. **101**, 081704 (2007).
[9] J. Schörmann, D. J. As, K. Lischka, P. Schley, R. Goldhahn, S. F. Li, W. Löffler, M. Hetterich, and H. Kalt, Appl. Phys. Lett. **89**, 261903 (2006).
[10] H. Lu, W. J. Schaff, L. F. Eastman, J. Wu, W. Walukiewicz, D. C. Look, and R. J. Molnar, Mater. Res. Soc. Symp. Proc. **743**, 317 (2003).
[11] H. Lu, W. J. Schaff, L. F. Eastman, J. Wu, W. Walukiewicz, V. Cimalla, and O. Ambacher, Appl. Phys. Lett. **83**, 1136 (2003).
[12] Y. Nanishi, Y. Saito, T. Yamaguchi, M. Hori, F. Matsuda, T. Araki, A. Suzuki, and T. Miyajima, Phys. Status Solidi A **200**, 202 (2003).
[13] P. D. C. King, T. D. Veal, P. H. Jefferson, C. F. McConville, H. Lu, and W. J. Schaff, Phys. Rev. B **75**, 115312 (2007).
[14] S. A. Chambers, T. Droubay, T. C. Kaspar, and M. Gutowski, J. Vac. Sci. Technol. B **22**, 2205 (2004).
[15] F. Fuchs, J. Furthmüller, F. Bechstedt, M. Shishkin, and G. Kresse, Phys. Rev. B (to be published), e-print arXiv:cond-mat/0604447v2.
[16] L. F. J. Piper, T. D. Veal, M. Walker, I. Mahboob, C. F. McConville, H. Lu, and W. J. Schaff, J. Vac. Sci. Technol. A **23**, 617 (2005).
[17] T. D. Veal, L. F. J. Piper, W. J. Schaff, and C. F. McConville, J. Cryst. Growth **288**, 268 (2006).
[18] G. Paasch and H. Übensee, Phys. Status Solidi B **113**, 165 (1982).
[19] B. R. Nag, *Electron Transport in Compound Semiconductors* (Springer, Berlin, 1980), p. 60.
[20] W. Mönch, *Semiconductor Surfaces and Interfaces*, 4th ed. (Springer, Berlin, 2001), p. 41.
[21] P. D. C. King, T. D. Veal, C. F. McConville, F. Fuchs, J. Furthmüller, F. Bechstedt, J. Schörmann, D. J. As, K. Lischka, Hai. Lu, and W. J. Schaff (unpublished).
[22] B. R. Nag, Phys. Status Solidi B **237**, R1 (2003).
[23] C. Stampfl and C. G. Van de Walle, Phys. Rev. B **57**, R15052 (1998).
[24] X. H. Lu, P. Y. Yu, L. X. Zheng, S. J. Xu, M. H. Xie, and S. Y. Tong, Appl. Phys. Lett. **82**, 1033 (2003d).
[25] M. Murayama and T. Nakayama, Phys. Rev. B **49**, 4710 (1994).

Downloaded 27 Jan 2009 to 130.236.174.69. Redistribution subject to AIP license or copyright; see http://apl.aip.org/apl/copyright.jsp